STEADY STATE SIMULATION OF A ROTARY KILN FOR CHARCOAL ACTIVATION

O. A. ORTIZ, N. D. MARTINEZ, C. A. MENGUAL and S. E. NORIEGA

Instituto de Ingeniería Química, Univ. Nac. de San Juan, 5400 – San Juan, Argentina.
rortiz@unsj.edu.arT

***Abstract*— This work presents a mathematical modeling and steady state simulation study of the pilot scale rotary kiln behavior, which was designed to activate charcoal obtained from the raw materials of region of Cuyo-Argentina. The proposed model aims for acquiring useful information to select operating conditions and design parameters. It is a simplified mathematical model that consists of a system of non-linear differential and algebraic equations, including a simple kinetic expression as well. Its solution, using the finite differences method, allows for obtaining solid flow rate, solid temperature, gas, and wall temperature profiles under a variety of operation conditions and as a function of the kiln's length. Parameters such as burn off and production yield were analyzed and the results were compared with characteristic data taken from the literature. This model, once adjusted with experimental data, will allow to adjust the kiln's operation in order to optimize both the energy usage and product quality.**

***Keywords*— rotary kiln, activated carbon, activation, modeling, simulation.**

I. INTRODUCTION

Activated carbon (AC) is a well known adsorbent material, which finds its usage in chemical, mining and food industries, and in other important applications such as purification and deodoration processes, water treatment, and medicine as well (Yehaskel, 1978; Bansal et al.,1988). In Argentina, there is an increasing interest in the development of a technology to cope with the local demand.

Much research on activated carbon has been undertaken at the National University of San Juan-Argentina during the last decade, such as coal gasification, production of AC by chemical and physical activation from several raw materials and AC characterization (Deiana et al., 1998). Using those data, approximate kinetic expressions were also developed (Martínez, 1998). Besides, a pilot-scale rotary kiln was built to study the physical activation of charcoal obtained from regional raw materials.

Although rotary kilns are widely used by the chemical industry, they still remain among the pieces of equipment most difficult to be properly analyzed due to the complexity of internal phenomena (e.g., heat, mass, and momentum transfer) along with the eventual chemical reaction phenomena (Barr et al., 1989). Rotary kilns are used by almost all the most important AC world manufacturers (Norit & Co.). However, studies about the modeling of processes to activate charcoal with steam in rotary kilns have not been published. Due to the specificity arising from each raw material and the difficulties associated with proposing general-type kinetics for the process, there are not published studies of the activation reaction kinetics, either. Thus, the majority of published works on activation and re-activation at pilot scale are empirical (Smith,1979; Laine et al., 1991) and a mathematical model to predict the stationary and dynamic performance of rotary kilns for the activation of charcoal is lacking at present.

The present work introduces mathematical modeling of the steady state operation of such a kiln, aiming to obtain valuable information for the proper selection of operating conditions and design parameters.

The achieved results allow for gaining understanding about the rotary kiln steady state performance. Such information, together with experimental data and the study of the process dynamics will allow for the proper kiln operation and control.

II. PILOT ROTARY KILN

A pilot rotary kiln is basically a cylinder which rotates around its longitudinal axis and operates essentially as a heat exchanger. The cylinder is lightly inclined (i.e., slope about 2-6%) to facilitate the axial displacement of the solid bed, which moves towards the discharge end as the hot gases circulate counter-current mode. Figure 1 shows an outline of the rotary kiln. The solid feed is a carbonized matter obtained from a variety of raw materials (e.g., eucalyptus wood). The hot gases, which arise from a central burner and are originated by combustion of natural gas, supply the necessary energy for the activation reaction. Steam is used as the activation agent and is injected in co-current mode.

Most of the raw materials are relatively pure solids, with moisture contents around 5 to 10%. Raw material grain size was -6+20#ASTM, which is equivalent to an average particle size of 0.002 meter. Usually, the content of impurities in the carbonized solid was negligible.

It is supposed that the solid bed moves as a pseudo fluid with axial displacement and without retro - mixing, and it rolls or slides in traverse direction as the cylinder rotates.

The geometric parameters (i.e., L_{cs}, L_{cu} and L_{li}) were determined as a function of the solid flow rate, residence time, and rotary kiln dimensions, by means of geometric relationships and iterative calculation (Coul-

son and Richardson, 1981; Wilbrand, 1997). Equation 1, which satisfactorily predicts residence times in rotary kilns (Perry et al., 1984) was used in this work.

$$t = \frac{0.19\ L}{N\ D_i\ S} \qquad (1)$$

III. MATHEMATICAL MODEL

There are three phases inside a rotary kiln: gas, solid, and wall. Beside the activation chemical reaction, the phenomena occurring are: mass transfer (i.e., solid's moisture and gaseous reaction products are transferred from the solid to the gas phase) and heat transfer (i.e., convection and radiation between gas and solid bed, gas and wall, wall and solid bed, and wall and surroundings, and conduction inside of the wall).

In order to model the transfer phenomena for the existing phases, the differential mass and energy balances, which include chemical reaction terms, are posed in cylindrical coordinates. Based on laboratory tests, publications on the subject (Wilbrand, 1997; Kim and Srivastava, 1990), and geometric characteristic, the following assumptions were adopted:

- Both, solid and gas axial linear velocity changes are negligible.
- All variables are supposed uniform in the radial direction due to the small size of the reactor.
- There is neither solid nor gas axial mixing. Then, the two phases are considered as a plug flow model. Solid drag by gas is negligible.
- Variations in rotary kiln wall temperature in the angular direction are neglected. (i.e., the so called regenerative effect of the wall).
- Constant steam flow rate is assumed.
- Pressure in the reactor is constant.
- Chemical reaction rate obeys the Arrhenius law, and secondary reactions are rejected.
- Axial heat transfer by conduction and radiation is negligible.
- Axial heat transfer by conduction inside the wall is unimportant.
- Specific heats, reaction heat, heat of vaporization, emissivities, absorptivities, and heat transfer coefficients by conduction in the wall, are supposed constant and temperature independent.

A. Chemical reaction rate

Equation 2 shows the solid disappearance, a consequence of the chemical reaction between carbonaceous material and steam (Yehaskel, 1978). In order to obtain the kinetic expression, the secondary reactions which occur in the reactor are not considered. The secondary reaction, formation of CO_2 from CO and steam, has not been taken account since it is a reversible reaction produced into an environment containing high CO_2 concentration because of the combustion of heating gases.

$$C + H_2O \ ==> CO + H_2 \ [28{,}5\ Kcal / mol] \qquad (2)$$

A kinetic equation responding to the Arrhenius law was obtained from laboratory data measured under experimental conditions similar to those of the rotary kiln operation (Martínez, 1998). Considering the steam flow rate constant, the reaction becomes pseudo first order: The obtained expression was modified in order to adapt it to the mass balance given as the mass flow rate variation along the z-coordinate.

$$r_s = -\frac{\partial Q_s}{\partial z} = \frac{6.005\left[\exp\left(-8033/T_s\right)\right] Q_a\ Q_s}{V_s} \qquad (3)$$

B. Mass balance for moisture in the solid bed

The drying of solids has a first stage governed by the evaporation rate, and it is considered that the solid surface remains saturated. In a second stage, the drying process is governed by diffusion of moisture from inside of the particle toward its surface (Coulson and Richardson, 1981). For critical moisture of 10% and supposing the continuity of the two stages, the moisture variation of the solid in the axial direction can be expressed by Eqn. 4 (see Table 1).

C. Mass balance for the solid bed

The solid moves through the reactor in the positive

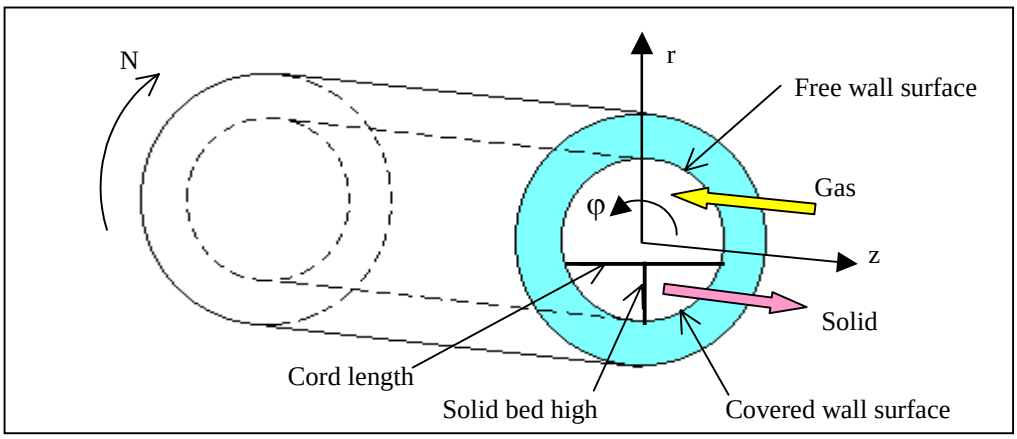

Figure 1. Reactor scheme and cross section.

Table 1. Equation system for the proposed model

- Mass balance for the solid's moisture: $$\frac{\partial Q_h}{\partial z} = -\frac{h_t \cdot A \cdot (T_g - T_s) \cdot Q_h}{H_v \cdot (0.1 \cdot Q_s)} \quad (4)$$

- Mass balance for the solid: $$\frac{\partial Q_s}{\partial z} = -k_e \cdot e^{-\left(\frac{8033}{Ts}\right)} \cdot Q_a \cdot \frac{Q_s}{V_s} - \frac{h_t \cdot A \cdot (T_g - T_s) \cdot Q_h}{H_v \cdot (0.1 \cdot Q_s)} \quad (5)$$

- Mass balance for the gas: $$\frac{\partial Q_g}{\partial z} = -k_e \cdot e^{-\left(\frac{8033}{Ts}\right)} \cdot \frac{Q_s}{V_s} \cdot Q_a \cdot \frac{30}{12} - \frac{h_t \cdot A \cdot (T_g - T_s) \cdot Q_h}{H_v \cdot (0.1 \cdot Q_s)} \quad (6)$$

- Energy balance for the gas: $$\frac{\partial (Q_g \cdot C_g \cdot T_g)}{\partial z} = -C_3 \cdot (T_g - T_s) - C_4 \cdot (T_g^4 \cdot e_g - T_s^4 \cdot A_v) - C_5 \cdot (T_g - T_w) - C_6 \cdot (T_g^4 \cdot e_g - T_w^4 \cdot A_v) + \frac{\partial Q_h}{\partial z} \cdot C_v \cdot (T_s - 373) \quad (7)$$

- Energy balance for the solid: $$\partial \frac{(Q_s \cdot C_s \cdot T_s)}{\partial z} = C_3 \cdot (T_g - T_s) + C_4 \cdot (T_g^4 \cdot e_g - T_s^4 \cdot A_v) + C_7 \cdot (T_w - T_s) + C_8 \cdot (T_w^4 \cdot e_g - T_s^4 \cdot A_v) - \frac{\partial Q_h}{\partial z} \cdot H_v - k_e \cdot e^{-\left(\frac{8033}{Ts}\right)} \cdot \frac{Q_s}{V_s} \cdot Q_a \cdot \Delta H \quad (8)$$

- Temperature at the internal wall: $$T_w = \frac{\left[\frac{T_a}{h_i \cdot R_i} + T_g \cdot \left[\frac{1}{\left[\left[1 + \frac{T_a}{T_{w0}} + \left(\frac{T_a}{T_{w0}} \right)^2 + \left(\frac{T_a}{T_{w0}} \right)^3 \right] \cdot e_{w0} \cdot \sigma \cdot (T_{w0})^3 + h_o \right] \cdot R_e} \right] - \frac{\ln \frac{R_i}{R_e}}{K_w} \right]}{\frac{1}{h_i \cdot R_i} + \frac{1}{\left[\left[1 + \frac{T_a}{T_{w0}} + \left(\frac{T_a}{T_{w0}} \right)^2 + \left(\frac{T_a}{T_{w0}} \right)^3 \right] \cdot e_{w0} \cdot \sigma \cdot (T_{w0})^3 + h_o \right] \cdot R_e} - \frac{\ln \frac{R_i}{R_e}}{K_w}} \quad (9)$$

- Temperature at the external wall: $$T_{w0} = T_w - \frac{[T_w - T_a] \cdot 0.693}{0.693 + \frac{k_w}{h_o \cdot R_e}} \quad (10)$$

- Heat transfer coefficient gas – internal wall: $$h_i = h_{gw} + \sigma \cdot e_g \cdot e_w \cdot \left(T_g^3 - T_w^3 \right) \quad (11)$$

direction of the z-coordinate. The solid flow rate variation along the reactor can be expressed by Eqn. 5 (see Table 1). The right term of this expression has two parts: the disappearance of solid by chemical reaction, according to Eqn. 3, and the loss of water by evaporation, according to Eqn. 4.

D. Mass balance for the gas phase

The gas flow rate increase in the negative direction of the z-coordinate is due to the appearance of water evaporated from the solid bed and the gases produced by chemical reaction. Gases and solids move along the rotary kiln in counter-current mode. This fact determines the sign of each term in Eqn. 6.

E. Energy balance for the gas phase

The gas heat flow variation along the z-coordinate depends on the heat transferred by convection and radiation between gas and solid and gas and wall, plus the required sensible heat to overheat the vapor from the boiling temperature (i.e., 373 K) to the freeboard gas temperature (see Eqn. 7 in Table 1). The parameters C_3, C_4, C_5 and C_6, which include heat transfer coefficients and heat transfer areas, are given in Table 2.

F. Energy balance for the solid phase

The solid heat flow variation along the z-coordinate depends on the heat transferred by radiation from solid to both gas and wall, the heat transferred by convection to gas and wall, the heat loosed as the solid's moisture evaporates, and the heat absorbed by the solid to chemically react (i.e., endothermic reaction, see Eqn. 8 in Table 1 and parameters C_7 and C_8 in Table 2).

G. Energy balance for the wall

It accounts for the heat transferred by conduction through the wall and the heat transferred by convection and radiation (gas-wall and wall- surroundings).

The heat transferred by conduction and convection between the covered wall (i.e., covered by the solid bed) and the solid itself was not considered because both phases, solid and wall, reach thermal equilibrium just in the first third of the kiln length.

The cyclic change in wall temperature was neglected (i.e., the so called regenerative effect) due to the small size of the kiln and because the high temperature zone covers the reactor length almost completely. In this zone, the main heat flow takes place fundamentally by radiation to the solid from both the gas and the not covered wall.

The internal wall temperature was necessary to solve the model. A complex system of equations was obtained after considering the net heat flow (i.e., gas-wall, internal-external wall and external wall-surroundings). In order to solve such system, the heat transferred by radiation was neglected and only the heat transferred by convection was considered. The radiation phenomenon was included in the convection heat transfer coefficient (Gorog et al., 1982).

The resulting equation for the internal wall temperature T_w (see Eqn. 9 in Table 1) include the external wall temperature, T_{wo}, which was calculated using the expression proposed by Gorog et al. (1982) (see Eqn. 10 in Table 1). The wall-surroundings heat transfer coefficient was included in Eqn. 9. The gas-wall heat transfer coefficient, h_i, is shown in Eqn. 11. This coefficient includes the heat transferred by both convection and radiation (McAdams, 1954).

Table 2. Equation parameters

$$C_3 = h_{gs} \quad L_{cu}$$

$$C_4 = \frac{\sigma \cdot L_{cu} \cdot e_s}{[1 - (1 - e_s)(1 - A_v)]}$$

$$C_5 = h_{gw} \quad L_{li}$$

$$C_6 = \frac{\sigma \cdot L_{li} \cdot e_w}{[1 - (1 - e_w)(1 - A_v)]}$$

$$C_7 = h_w \cdot L_{es}$$

$$C_8 = \sigma \cdot L_{cu} \cdot \phi_{sw} \cdot e_w \cdot e_s$$

$$\phi_{sw} = \left\{ \frac{1}{1 - e_g} - (1 - e_w) \cdot \left[\frac{L_{cu}}{L_{li}} \cdot (1 - e_s) + \left(1 - \frac{L_{cu}}{L_{li}} \right) \right] \right\}^{-1}$$

The parameters $C_3,\ldots, C_8$ in the model given in Table 1 are shown in Table 2. For the wall-solid convection heat transfer, h_w, the equation proposed by Wilbrand, (1997) was used. The gas-wall, h_{gw}, and gas-solid heat transfer coefficients, h_{gs}, were calculated by means of the expressions proposed by Gorog et al. (1982).

IV. RESULTS AND DISCUSSION

The proposed model which is constituted by a non-linear differential and algebraic equation system, was solved by means of the finite differences method. Although this resolution method is less exact than others (e.g., finite volumes) it is suitable for a one-dimensional simple geometry. Due to its user's friendly nature, the commercial software Mathcad 2000 Professional was used to solve the model.

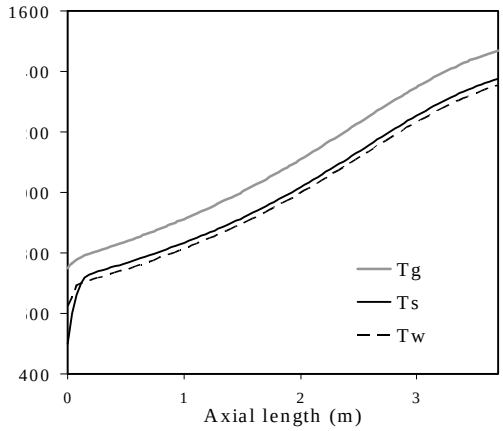

Figure 2. Temperature profiles of gas, wall and solid vs. axial length.

The model was applied to different operation conditions of the rotary kiln, and the results compared with experimental data.

The initial operation conditions at the rotary kiln input extreme, Q_{s0}, T_{s0}, Q_{g0}, T_{g0}, Q_{h0}, T_{w0}, Q_a and N, were known. Because the calculation starts at the solid input extreme, the output gas temperature was also supposed as an initial condition. The computation begins at z = 0 with the initial given conditions, and continues until z = L. Then, the calculated inlet gas temperature is compared with the actual data. If the convergence is not achieved, a new outlet gas temperature value is proposed. A Nelder and Mead (1965) optimization method has been used, and the rate of convergence was acceptable for the used initial conditions. Rotary kiln operation data and initial conditions assumed for the example case are reported in Table 3.

Figure 2 shows the temperature profiles of the solid (T_s), gas (T_g) and wall (internal, T_w, and external, T_{w0}) versus rotary kiln axial length. Since the simulation results could not be contrasted with our experimental data, the data reported by Barr et al. (1989) were taken as a reference. A complete set of experimental results for several endothermic reactions in a pilot rotary kiln is presented in this paper. The temperature profiles

Table 3. Equipmen characteristics and initial conditions.

Equipment characteristics	
Length and Internal Diameter:	3.7 m - 0.30 m
External Diameter:	0.60 m
Raw Material:	Solid carbonaceous material
Solids flow rate:	$\leq 3.9 \cdot 10^{-3}$ Kg.$\cdot s^{-1}$
Moisture content:	5 – 10 %
Particle size:	0.002 m (-6+20) # ASTM
Activation gas:	Steam
Steam Flow Rate:	$\leq 5 \cdot 10^{-3}$ Kg.$\cdot s^{-1}$
Reaction temperature:	1073 – 1273 K
Rotary Kiln Pressure:	Atmospheric
Rotational speed:	1 to 3 rpm
Rotary kiln inclination slope:	2 to 6 %
Residence time:	≤ 7200 s
Initial Conditions	
$Q_{s.0} = 3.33 \cdot 10^{-3}$ kg $\cdot s^{-1}$	
$Q_{g.0} = 3.5 \cdot Q_{s0}$	
$T_{s.0} = 500$ K	
$T_{g.0} = 750$ K	
rpm = 2	
t = 6480 s	

obtained with the proposed model fitted acceptably the experimental data reported in the literature (see Fig. 3). The solid flow rate variation, which was due to weight losses by reaction, along the axial length is shown in Fig. 4.

In order to analyze the production performance, two parameters were used: production yield and burn-off. The kiln's production yield was defined as the relationship between the solid flow rate at the output extreme and the solid flow rate at the input extreme (see Eqn. 12). The burn-off, which represents a measure of the activation reaction extent, was calculated as the relationship between the solid converted and the solid fed minus the moisture lost by the solid (see Eqn. 13).

$$\eta = \frac{Q_{s.Out}}{Q_{s0}} \quad 100 \tag{12}$$

$$Bo = \frac{Q_{s.0} \quad Q_{s.Out}}{Q_{s.0}} \quad 100 \tag{13}$$

For the particular case studied, the results for production yield and burn off were 72.5 % and 18.4 %, respectively. These results agree with those reported by Smith in 1979 for eucalyptus charcoal samples tested in a similar pilot rotary kiln. The average production yield and burn off published were 70 - 75% and 18 - 20%, respectively. Furthermore, the activated product obtained displayed very good adsorbent properties and an acceptable mechanical resistance. For a production yield

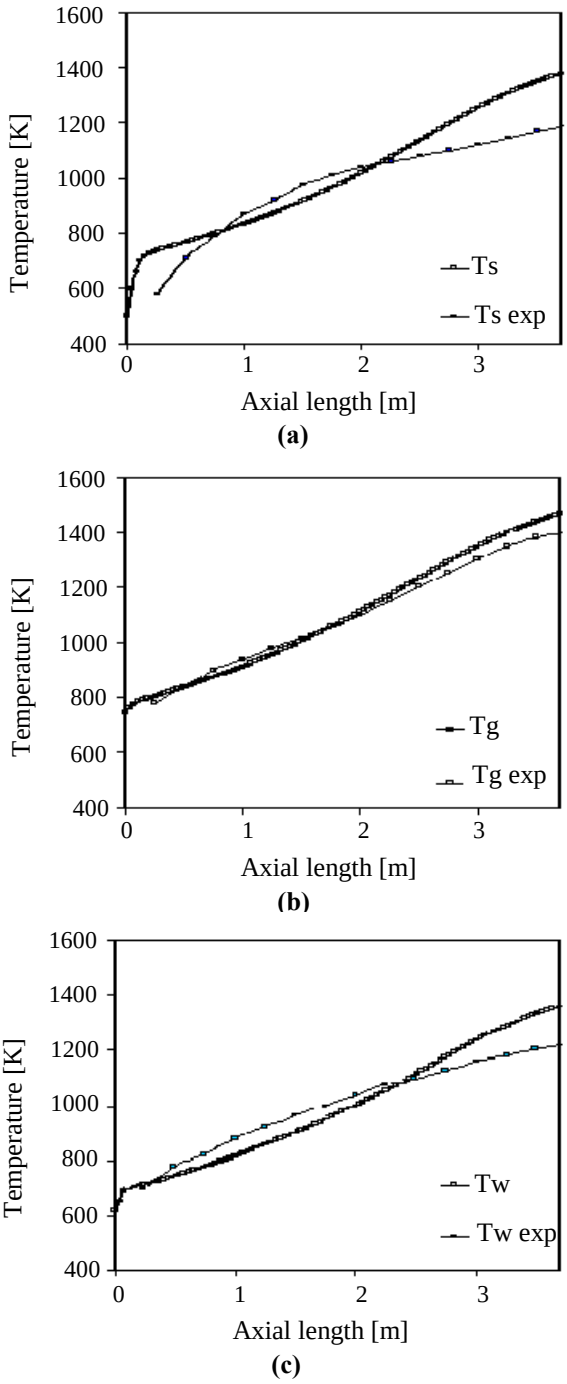

Figure 3. Profiles comparison of **(a)** solid, **(b)** gas and **(c)** wall temperature with bibliography experimental data.

of 75%, the results were: Iodine Number of 763 mg/g, Modified Phenol Value of 15.8 ppm and Abrasion Number of 54%.

V. CONCLUSIONS

Since the physical and the chemical processes which occur inside the rotary kiln are very complex, it was necessary to adopt different assumptions in order to develop a mathematical model that could be solved easily.

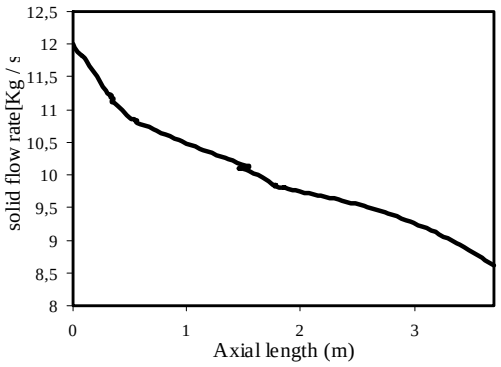

Figure 4. Solid flow rate vs. reactor axial length

Given the small size of the kiln and the operation conditions tested, the assumptions lead to a model whose resolution was of medium complexity when traditional mathematical methods were applied.

The mass transfer due to the chemical reaction was modeled using a simple kinetic equation generated from own experimental data. This allowed to simulate the mass transfer between solid and gas, properly.

An estimation of the heat transfer coefficients is quite difficult because of the lack of reliable experimental data. The relative importance of the heat transferred by radiation with respect to other transfer phenomena was also verified since the model was particularly influenced by changes in those coefficients.

The results obtained from the steady state simulation allowed to observe the effects of the heat and mass transfer, when the activation reaction was carried out. They also permitted to have a model that describes the kiln performance properly. Although the model should be adjusted to our experimental data, the comparison with characteristic experimental values from the literature was reasonably good. This occurred in spite of the model middle complexity and that the regenerative effect of the wall was not considered.

The model, once improved with our experimental data, will permit to adapt the operation conditions of the rotary kiln to reduce the energy consumption and to improve product quality. In a next paper, a performance analysis will be addressed to select the optimal operational conditions.

NOMENCLATURE

A	Gas-solid surface per unit of length [$m^2 \cdot m^{-1}$]
A_v	Absorptivity
C_g	Average specific heat of gas [$kJ \cdot kg^{-1} \cdot K^{-1}$]
C_s	Average specific heat of solid [$kJ \cdot kg^{-1} \cdot K^{-1}$]
C_v	Average specific heat of steam [$kJ \cdot kg^{-1} \cdot K^{-1}$]
D_i	Internal diameter [m]
e_g	Gas emisivity
e_s	Solid emisivity
e_w	Emisivity of internal surface of wall
e_{w0}	Emisivity of external surface of wall
h_{gw}	Heat transfer coefficient between the wall and gas [$W \cdot m^{-2} \cdot K^{-1}$]
h_0	Heat transfer coefficient between the wall and surrounding [$W \cdot m^{-2} \cdot K^{-1}$]
h_{gs}	Heat transfer coefficient between the solid and gas [$W \cdot m^{-2} \cdot K^{-1}$]
H_v	Latent heat of vaporization of water [$kJ \cdot kg^{-1}$]
ΔH	Heat of reaction [$kJ \cdot kmol^{-1}$]
k_e	First order reaction rate constant [s^{-1}]
k_w	Thermal conductivity of wall [$kW \cdot m^{-1} \cdot K^{-1}$]
L_{li}	Free wall surface [m^2]
L_{cs}	Covered wall surface [m^2]
L_{cu}	Cord length [m^2]
N	Rotational speed [rpm]
Q_a	Steam flow rate [$kg \cdot s^{-1}$]
Q_g	Gas flow rate [$kg \cdot s^{-1}$]
Q_h	Moisture flow rate [$kg \cdot s^{-1}$]
Q_s	Solid flow rate [$kg \cdot s^{-1}$]
r_s	Activation reaction rate (coal) [$kg \cdot s^{-1} \cdot m^{-1}$]
R_e	External radius of the cylinder [m]
R_i	Internal radius of the cylinder [m]
S	Rotary kiln inclination slope
T_a	Surrounding temperature [K]
T_s	Solid temperature [K]
T_g	Gas temperature [K]
T_w	Temperature of internal surface of the wall [K]
T_{w0}	Temperature of external surface of the wall [K]
V_s	Solid velocity [$m \cdot s^{-1}$]
ϕ_{sw}	Radiation number
σ	Boltzman constant $5.57.10^{-8}$ [$W \cdot m^{-2} \cdot K^{-4}$]

REFERENCES

Bansal, R., J. Donnet and F. Stoeckli, *"Active Carbon"*, Marcel Dekker Inc. (1998).

Barr P., J. Brimacombe and A. Watkinson, "A heat transfer model for the rotary kiln. Part I." *Pilot kiln trials, Metallurgical Transactions*, **20B**, 391-402 (1989).

Coulson, J. And J. Richardson, *"Ingeniería Química: Operaciones Básicas"*, Editorial Reverté S. A. (1981).

Deiana C., L. Petkovic and S. Noriega, "Carbón Activado a partir de Materias Primas Regionales", *Información Tecnológica* **9**, 5 (1998).

Gorog J.P., T.M. Adams and J.K. Brimacombe, "Regenerative Heat Transfer in Rotary Kilns", *Metallurgical Transactions B* **13B**, 153-163 June (1982).

Kim, N. and R. Srivastava, "Simulation and Control of an Industrial Calciner", *Ind. Eng. Chem. Res.* **29**, 71-81 (1990).

Laine J., S. Simoni and R. Calles, "Preparation of activated carbon from coconut shell in a small scale cocurrent flow rotary kiln", *Chemical Engineering Comm.* **99**, 15-23 (1991).

Martínez, N.,*"Ecuación Cinética para la activación de Carbón de Eucalipto"*, Internal Report (not published), Instituto de Ingeniería Química, Universidad Nacional de San Juan (1998).

Mc Adams, W.H., *"Transmisión de Calor"*, 1st Edition, McGraw Hill (1954).

Nelder, J.A. and R. Mead, "A Simplex Method for Function Minimization", *Computer J*., Vol .**7**, pp. 308-313 (1965).

Perry R. and D. Green, *"Chemical Emngineers´ Handbook"*, 6th Edition, McGraw Hill (1984).

Smith S., *"Activated Charcoal for Water Purification from Florida Woods"*, Final Report Project A-2214 (1979).

Yehaskel A., *"Activated Carbon : Manufacture and Regeneratión"*, Noyes Data Corporation (1978).

Wilbrand K., "Thermische Boden-behandlung in Drehrohr-Verbrennungsanlagen- Simulation und Messung", *Fortschritt-Berichte VDI*, *Reihe* 15, Umwelttechnik, Nr. **170** (1997).